https://doi.org/10.5194/egusphere-2026-1992
Preprint. Discussion started: 30 April 2026

From Single Compounds to Ambient Aerosols: A Machine-Learning-Based Estimation of Organic Hygroscopicity

Shravan Deshmukh[1], Laurent Poulain[1], Birgit Wehner[1], Silvia Henning[1], Hartmut Herrmann[1], Mira Pöhlker[1,2]

[1]Leibniz Institute for Tropospheric Research, e.V. (TROPOS), Permoserstrasse 15, 04318 Leipzig, Germany
[2]Faculty of Physics and Earth Sciences, Leipzig Institute for Meteorology, Leipzig University, 04103 Leipzig, Germany

Correspondence to: Laurent Poulain (poulain@tropos.de), Silvia Henning (henning@tropos.de), and Mira Pöhlker (poehlker@tropos.de)

Abstract. Aerosol hygroscopicity strongly governs particle size, mixing state, and radiative effects, yet remains poorly constrained for organic aerosols due to their chemical complexity and limited observations. Here, we present laboratory-measured size-segregated hygroscopic properties of 22 organic compounds, including carboxylic acids, amino acids, sugars, and alcohols, using a hygroscopic tandem differential mobility analyzer (HTDMA) combined with chemical characterization by Aerosol Mass Spectrometry (AMS). Our results extend previous studies by resolving hygroscopic behaviour across the submicrometer size range most relevant to atmospheric processes and by systematically linking organic hygroscopicity (κ_{org}) across functional groups, as measured by AMS, with physicochemical properties. Structurally similar compounds may exhibit markedly different hygroscopic behavior, underscoring the role of molecular interactions. Similar to carbon chains, increased functionalization generally enhances hygroscopicity and induces a pronounced size dependence. Functional-group-based classifications from the AMS provide a useful approximation for estimating κ_{org}, but may not capture this complexity. Leveraging these laboratory constraints, we use a simple but extensible machine-learning framework that integrates laboratory-derived κ_{org} with ambient aerosol observations. The application of this hybrid approach to urban and rural environments demonstrates substantial improvements in predicting ambient hygroscopicity, with R^2 values increasing from 0.82 to 0.96 at the Paris suburban site SIRTA (France) and from 0.60 to 0.94 at the rural background site Goldlauter (Germany), compared to conventional composition-based models. By bridging controlled laboratory measurements with data-driven ambient analysis, this study provides a rigorous pathway to improve the representation of the direct aerosol radiative effect in atmospheric and climate models.

Introduction

Atmospheric aerosols significantly impact the Earth's radiation budget, exerting both direct and indirect effects (IPCC, 2013; Rosenfeld et al., 2014; Li et al., 2016). The ability of aerosol particles to interact with atmospheric water vapor depends strongly on their hygroscopic properties, which determine their growth under humid conditions and their potential to act as cloud condensation nuclei (CCN) (Petters and Kreidenweis, 2007). In addition to their climate effects, aerosol-water interactions also influence air quality, atmospheric chemistry, and human health (Ren et al., 2021; Li et al., 2022). A robust understanding of aerosol hygroscopicity is therefore essential for improving the representation of aerosol-cloud interactions and radiative forcing in atmospheric models. Atmospheric aerosols consist of complex mixtures of inorganic salts and organic compounds. While inorganic species such as ammonium sulfate, ammonium nitrate, and sodium chloride exhibit relatively well-characterized hygroscopic behavior, organic aerosols remain considerably more challenging to describe due to their chemical complexity (Estillore et al., 2016; Nakao, 2017). These organic species are of both anthropogenic and biogenic origin, often contribute a significant fraction (approximately 20% to 90%) to the mass of submicrometer aerosols, and have significant effects on air quality and climate (Jimenez et al., 2009; Han et al., 2022). It undergoes continuous physical and chemical transformations during its atmospheric lifetime. Consequently, their hygroscopic properties depend on a variety of molecular

https://doi.org/10.5194/egusphere-2026-1992
Preprint. Discussion started: 30 April 2026

characteristics, including functional groups, carbon number, oxygen content, and oxidation state (Han et al., 2022; Tan et al., 2024). This chemical diversity makes it difficult to represent organic aerosol hygroscopicity using simplified parameterizations.

The hygroscopic behaviour of organic aerosols is commonly described using the κ-Köhler framework, in which the hygroscopicity parameter κ provides a convenient representation of particle water uptake (Petters and Kreidenweis, 2007). For mixed inorganic-organic aerosols, the Zdanovskii–Stokes–Robinson (ZSR) mixing rule is frequently used, in which the total hygroscopicity is estimated as the volume-weighted sum of the individual components hygroscopicity. In many atmospheric modelling studies, the organic fraction is represented by a constant hygroscopicity parameter (e.g., $\kappa_{org} \approx 0.1$), while the inorganic components are assigned well-known κ values (Jiang et al., 2025). Although this approach provides a practical approximation, it neglects the large variability in organic hygroscopicity observed in laboratory and field measurements. As a result, assuming a constant κ_{org} can introduce systematic biases when predicting aerosol hygroscopic growth and CCN activity, particularly in environments where organic aerosols dominate the particle mass. Moreover, hygroscopic growth depends on particle size, and size-resolved κ_{org} can influence aerosol optical properties by altering particle diameter and scattering efficiency under humid conditions (Li et al., 2022). Accurately representing κ_{org} across relevant submicron particle sizes is therefore important for improving estimates of aerosol radiative effects.

A number of experimental studies have attempted to improve the understanding of κ_{org} by investigating individual compounds or specific compound classes. Laboratory measurements using hygroscopic tandem differential mobility analyzers (HTDMAs) have shown that molecular properties, such as solubility, functional groups, and oxidation state, strongly influence particle hygroscopicity (Han et al., 2022). Complementary approaches have also been developed to relate measured aerosol hygroscopicity to chemical composition in complex mixtures, including analyses of filter samples and offline chemical characterisation (Raparthi et al., 2025). While these studies have provided valuable insights, limitations remain. Many investigations focus on a limited number of compounds or one particle size and often lack a systematic framework for translating laboratory-derived relationships into predictive tools applicable to ambient aerosol observations. In addition, the variability of organic hygroscopicity across different particle sizes within the atmospherically relevant submicron range remains insufficiently constrained. Because thousands of organic compounds contribute to atmospheric aerosol, representing their individual hygroscopic behavior is impractical. Grouping compounds into functional families provides a simplified yet physically meaningful framework that captures dominant chemical characteristics while remaining computationally tractable for modelling. Recent advances in data-driven methods can address these challenges. Machine-learning (ML) approaches are increasingly used in atmospheric science to capture complex, nonlinear relationships between aerosol composition and physicochemical properties that are difficult to represent with traditional parameterizations (Bordoni et al., 2025; Chen et al., 2022). When combined with physically informed constraints, such approaches offer a promising pathway to link laboratory measurements with ambient observations and to improve the representation of aerosol hygroscopicity in models. Aerosol hygroscopicity is a key parameter in atmospheric models, but uncertainty due to organics persists, and it is important to reduce this knowledge gap.

https://doi.org/10.5194/egusphere-2026-1992
Preprint. Discussion started: 30 April 2026

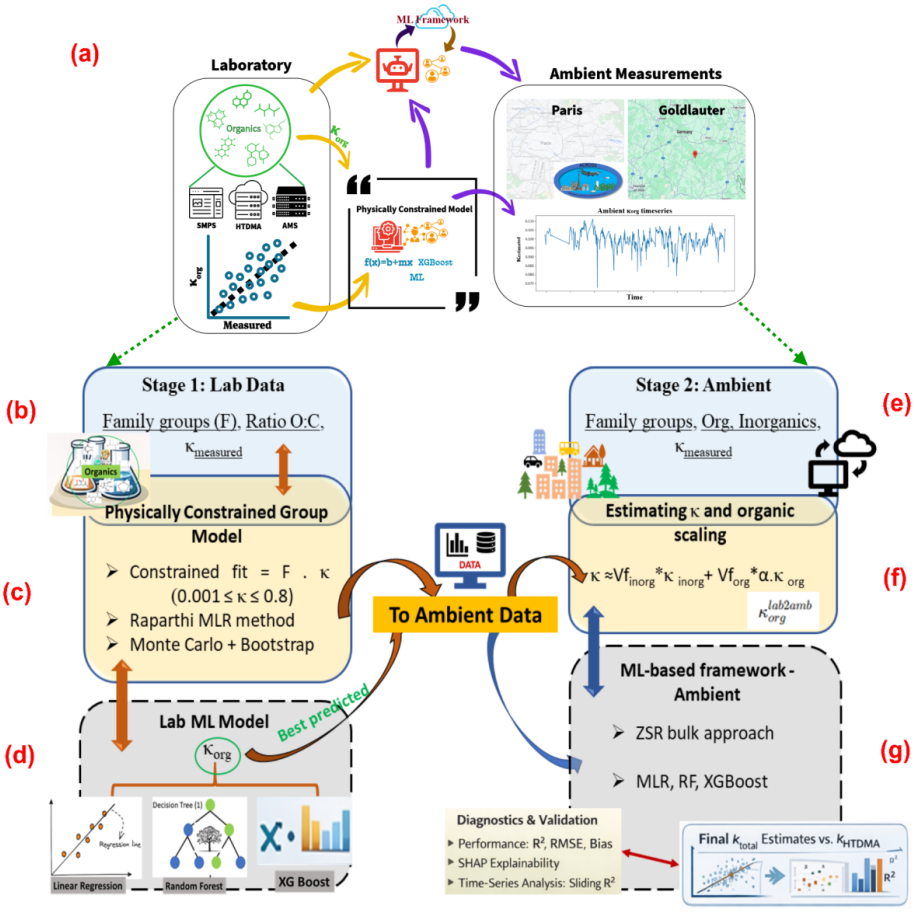

Figure 1: (a) Conceptual overview of the laboratory-constrained machine-learning framework and its application to ambient aerosol hygroscopicity. Laboratory measurements of 22 organic compounds using HTDMA and AMS are used to derive κ_{org} and train ML models. Then, a machine-learning framework is applied to ambient aerosol chemical composition at field sites (Paris and Goldlauter, from © Google Maps) to estimate time-resolved κ_{org} under real atmospheric conditions. Detailed stages of framework described as (b) laboratory dataset comprising organic family-group descriptors (F: $C_xH_y^+$, $C_xH_yO^+$, $C_xH_yO_{z=1}^+$) together with O:C and HTDMA-derived $\kappa_{measured}$. (c) Physically constrained group model used to infer group κ values by fitting $\kappa \approx F \cdot \kappa$ with bounds ($0.001 \leq \kappa \leq 0.8$), incorporating a Maximum A Posteriori regularization based on the (Raparthi et al., 2025) parameterization and uncertainty quantification via Monte Carlo sampling and bootstrapping. (d) Supervised lab ML models (MLR, Random Forest, XGBoost) trained on the laboratory descriptors to predict κ_{org}; the best-performing predictor is transferred to ambient data. (e) Ambient inputs include family groups and AMS-derived organic and inorganic components with $\kappa_{measured}$ (from HTDMA). (f) Effective inorganic hygroscopicity (κ_{inorg}) and an organic scaling factor (α) are estimated using a bulk mixing constraint, using their mass fractions and individual κ (κ_{org} information from lab-to-ambient). (g) Ambient $\kappa_{total=estimated}$ is evaluated using both a ZSR bulk approach and ML-based models, with diagnostics and a validation metric. The background maps are from © Google Maps.

In this context, the objective of this study is to develop a physically informed framework that bridges laboratory measurements of organic aerosol hygroscopicity with a predictive ML framework of ambient aerosol behavior (see Fig. 1). First, we perform laboratory measurements of hygroscopic growth for organic compounds using HTDMA across atmospherically relevant submicron particle sizes. We derive size-resolved hygroscopicity parameters (κ) for a diverse set of organic compounds from these experiments. Second, investigate how molecular properties and functional-group composition influence κ_{org} and evaluate whether simplified descriptors based on organic family groups can serve as effective predictors of organic hygroscopicity. Third, developing a machine-learning framework, augmented with Monte Carlo uncertainty analysis, to predict κ_{org} using molecular and compositional descriptors derived from laboratory observations. Leveraging these laboratory constraints, we use a simple machine-learning framework that integrates laboratory-derived κ_{org} with ambient aerosol observations. This laboratory-derived framework is applied to ambient aerosol observations from urban and rural environments, specifically Paris

https://doi.org/10.5194/egusphere-2026-1992
Preprint. Discussion started: 30 April 2026

(France) and Goldlauter (Germany). By integrating laboratory constraints with ambient chemical measurements, we demonstrate that the proposed approach improves the prediction of ambient aerosol hygroscopicity compared with conventional composition-based models that assume constant organic hygroscopicity. This hybrid methodology provides a pathway for representing κ_{org} variability in atmospheric aerosol systems and highlights the potential of combining laboratory experiments with data-driven modelling to improve the representation of aerosol hygroscopicity in atmospheric and climate models.

2 Methodology

2.1 Laboratory and ambient measurement

2.1.1 Laboratory setup measurements

Submicrometer aerosol particles were generated by nebulizing aqueous solutions (0.1 g L^{-1}) of each compound using a constant output atomizer. The solutions were prepared by using ultrapure water (Millipore, resistivity ≥ 18.2 MΩ). The physicochemical properties of the 22 studied compounds are summarized in Table 1 & S1. After particle generation, the particles were introduced into a TROPOS-style Mobility Particle Size Spectrometer (MPSS), Aerodyne High-Resolution Time-of-Flight Aerosol Mass Spectrometer (HR-ToF-AMS), referred to as AMS (DeCarlo et al., 2006), and the TROPOS-custom-built HTDMA was used to measure the hygroscopic growth factors of aerosol particles (Massling et al., 2007; Wu et al., 2013). The rough setup is illustrated in Fig. 1 under laboratory analysis.

Table 1. Properties of organic compounds used in this study: the most important atmosphere-relevant compounds are mentioned here, and all other compounds are listed in the supplementary Table S1.

Molecular Structure	Compounds	Chemical formula	Molar weight (g mol^{-1})	Density (g cm^{-3})	Solubility (g mL^{-1})	O/C	Hygroscopic growth (Measured)
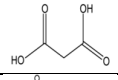	Malonic acid[1]	$C_3H_4O_4$	104.06[a]	1.62[a]	0.763[b]	1.33	1.48
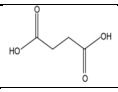	Succinic acid[1]	$C_4H_6O_4$	118.09[a]	1.19[a]	0.083[b]	1	1
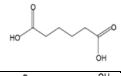	Adipic acid[1]	$C_6H_{10}O_4$	146.14[a]	1.36[a]	0.03[b]	0.67	1
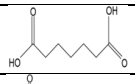	Pimelic acid[1]	$C_7H_{12}O_4$	160.17[a]	1.33[a]	0.05[b]	0.57	1.02
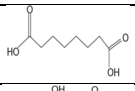	Suberic acid[1]	$C_8H_{14}O_4$	174.19[a]	1.3[a]	0.0006[a]	0.5	0.93
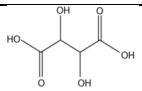	Tartaric acid[1]	$C_4H_6O_6$	150.09[a]	1.79[a]	1.43[c]	1.5	1.36
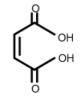	Maleic acid[1]	$C_4H_4O_4$	116.07[a]	1.59[a]	0.79[a]	1	1.36
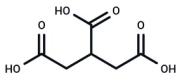	Tricarballylic acid[1]	$C_6H_8O_6$	176.12[a]	1.37[a]	0.05[a]	1.33	1.3

https://doi.org/10.5194/egusphere-2026-1992
Preprint. Discussion started: 30 April 2026

Supplier purity:[1]Sigma Aldrich, ≥ 99 %, [2]Fluka, 98%. [a]https://www.chemicalbook.com/ (last access: 05 December 2025). [b]https://pubchem.ncbi.nlm.nih.gov/ (last access: 05 December 2025). [c](Peng et al., 2001).

2.1.2 Ambient measurements

Field measurements used in this study were performed at the SIRTA observatory (Site Instrumental de Recherche par Télédétection Atmosphérique, http://sirta.ipsl.fr) located approximately 23 km southwest of the Paris city center (Haeffelin et al., 2005) on the Saclay plateau (2.148° E, 48.708° N; 150 m a.s.l.). One month of measurements from 16th June 2022 to 15th July 2022 during the ACROSS (Description – Across, n.d.) campaign was used. This "supersite" is surrounded by suburban facilities, forests, agricultural fields, and roads connecting Paris (Petit et al., 2015). It is part of the European Research Infrastructure for the observation of Aerosol, Clouds, and Trace gases, known as ACTRIS (Laj et al., 2024). Further, it is considered a representative of background conditions in the Paris region, with a detailed site description that can be found in (Deshmukh et al., 2025).

Another dataset was used from the measurement campaign, which took place in Goldlauter, Thuringia, central Germany, from September to October 2010, as part of the Hill Cap Cloud Thuringia (HCCT) project at the Schmücke research site. The results and description had been previously published by (Wu et al., 2013).

2.2 Hygroscopic growth, data inversion, and particle size measurements

A custom-built HTDMA was used to measure the hygroscopic growth factor of laboratory organic compounds and ambient aerosol particles. The polydisperse aerosol was first dried by passing it through a Nafion aerosol dryer and brought to charge equilibrium using an ^{85}Kr bipolar neutralizer. The selected dry diameters D_{dry} at specific narrow size fractions, centered around 100, 150, 200, and 250 nm, were measured in a differential mobility analyzer (DMA-1) and exposed at a relative humidity (RH) of 90 ± 3% (Bezantakos et al., 2013; Wu et al., 2013). Both DMAs were operated with a sheath flow rate of 5 L min^{-1} and a sample flow rate of ~1 L min^{-1}. It is worth noting that RH variance may have a measurable impact on GF, particularly for low-soluble compounds and those sensitive to RH, and could contribute to uncertainty, especially for organics. Although the RH calibration was maintained carefully using 100 nm pure ammonium sulfate particle measurements, this uncertainty is acknowledged as a potential source of error in our measurements, as well as in ambient measurements from different sites of HTDMA data, and has been presented in previous studies through corresponding original publications (Deshmukh et al., 2025; Wu et al., 2013).

The hygroscopic growth factor (GF) determined by the HTDMA is the ratio of the humidified (D_{wet}) and dry (D_{dry}) particle mobility diameter at a given RH in Eq. (1):

$$GF = \frac{Dwet}{D_{dry}}, \quad (1)$$

The TDMAinv method developed by (Gysel et al., 2009) was used to invert the data. The residence time of particles at RH (90 %) before entering the DMA-2 is estimated to be approximately 2.5 seconds in the TROPOS-HTDMA system (Wu et al., 2013). The short residence time could introduce an additional bias in measurements of particles dominated by organics (Peng & Chan, 2001; Chan & Chan, 2005; Sjogren et al., 2007; Duplissy et al., 2009). The hygroscopicity parameter (κ) can be computed using the hygroscopic growth factor (GF) measured through an HTDMA, based on (Stokes & Robinson, 1966) and outlined by (Gysel et al., 2007).

$$\kappa_{measured} = (GF^3 - 1)\left(\frac{exp\left(\frac{A}{D_{dry} \cdot GF}\right)}{RH} - 1\right), \quad (2)$$

https://doi.org/10.5194/egusphere-2026-1992
Preprint. Discussion started: 30 April 2026

$$A = \frac{4\,\sigma_{s/a}\,M_w}{RT\rho_w}, \quad (3)$$

D_{dry} and GF are the initial dry particle diameter and hygroscopic growth factor at 90 % RH measured by HTDMA. $\sigma_{s/a}$ is the droplet surface tension (assumed to be that of pure water, $\sigma_{s/a}$ = 0.0728 N m^{-2}), M_w the molecular weight of water, ρ_w the density of liquid water, R the universal gas constant, and T the absolute temperature.

Alternatively, for ambient measurements, κ_{chem} can be predicted using a simple mixing rule based on chemical volume fractions (V_fi), as proposed by (Petters and Kreidenweis, 2007):

$$\kappa_{chem} = \sum_i V_f i \,.\, \kappa_i \quad (4)$$

Here, κ_i and V_fi are the hygroscopicity parameter and volume fraction of the i-th component in the mixture, respectively. The respective sites used the chemical composition from the AMS and AE33 (black carbon) measurements. The approach we used to predict κ_{chem} follows the Zdanovskii-Stokes-Robinson (ZSR) mixing rule. To some extent, we indirectly incorporate solubility and chemical composition information into κ calculations, particularly for particles with organic fractions exceeding 50%. Hence, in ZSR-based κ predictions, the values of κ_i used in this study (see Table 2) are based on literature-measured values with some water activity calculation (Deshmukh et al., 2025) and uncertainties in the datasets are already accounted for. Changing κ_i in calculations doesn't significantly change κ_{chem} prediction, as lower soluble compounds like organics generally show only slight hygroscopic growth at relative humidities less than 98% (Petters et al., 2009; Wex et al., 2009).

During the laboratory investigation, the TROPOS-style MPSS is operated concurrently with the HTDMA and AMS at aerosol-to-sheath flow ratio of 1:5 L min^{-1}. Both aerosol and sheath flows were dehydrated to a relative humidity lower than 40% using a Nafion dryer. In laboratory experiments, MPSS was used to size-select AMS and was run at fixed sizes (i.e., 100, 150, 200, and 250nm) to provide a similar size selection to that used for the hygroscopicity measurements.

Table 2. Gravimetric densities ρ and hygroscopicity parameters κ at the sub-saturated regime used in this study.

Species	NH_4NO_3	H_2SO_4	NH_4HSO_4	$(NH_4)_2SO_4$	Organic matter	Black carbon
ρ (kg m^{-3})	1720[a]	1830[a]	1780[a]	1769[a]	1400[a, c]	1770[a, b]
κ	0.58[a]	0.9[a, b]	0.56[a]	0.48[a]	0.1[a, c]	0

[a](Gysel et al., 2007, 2011); [b](Kondo et al., 2011; Park et al., 2004; Wu et al., 2013); [c](Alfarra et al., 2006; Dinar et al., 2006)

2.3 Chemical composition and family group measurements

The Aerodyne HR-ToF-AMS (referred to as AMS) was typically operated with a time resolution of 2 minutes. The AMS, owing to the vaporizer's 600°C surface temperature (DeCarlo et al., 2006), exclusively analyses the non-refractory chemical composition of particles, limiting its ability to detect soot, crustal material, and sea salt. Consequently, based on the aerodynamic lens transmission efficiency and the identified compounds, the AMS provides the chemical composition of the sub-micrometer non-refractory aerosol fraction at NR-PM1 (Canagaratna et al., 2007). The combination of hot vaporization and ionization at 70eV leads to significant fragmentation of the organic species, making the identification of individual species quasi-impossible; however, different approaches can be used to depict the change in the organic mass spectra over time. One of them consists of grouping the different organic fragments into specific, so-called families and investigating changes in the distribution of these families over time. One family (e.g., C_x^+, $C_xH_y^+$, $C_xH_yO^+$, $C_xH_yO_z^+$, where x represents the number of C atoms, y the number of H atoms, and z > 1 the number of O-atom in the fragments) represents the sum of the organic fragments having

https://doi.org/10.5194/egusphere-2026-1992
Preprint. Discussion started: 30 April 2026

different combinations of C, H, and O that define the family. Additionally, utilising the approach developed by (Aiken et al., 2008) and further improved by (Canagaratna et al., 2015), high-resolution organic particle mass spectra were employed to determine the elemental composition and the oxygen-to-carbon (O:C) atomic ratio. The uncertainty in chemical composition for AMS varies across chemical species and is reduced using calibration collection efficiency (CE) for the system. For these measurements, the ion CE was $4.44e^{-08}$, and based on this, the uncertainty in the chemical composition was roughly estimated at 10-15%.

2.4 Machine learning framework

We develop a two-stage, composition-explicit framework to quantify organic hygroscopicity (κ_{org}) with comparison to ambient hygroscopicity ($\kappa_{measured}$). A laboratory hygroscopicity and composition measurements of 22 standard organic compounds were used to train a machine learning (ML) framework of κ_{org} predictors, including linear regression, Random Forest Regression (RFR or RF), and Extreme Gradient Boosting (XGBoost) models, utilizing molecular family descriptors (C_x^+, $C_xH_y^+$, $C_xH_yO^+$, $C_xH_yO_z$, and O:C ratios). These data were complemented with a physically constrained κ parameterization model, Eq. 12 (κ = 0.163 (O/C) + 0.022 C + 0.037 O* + 0.119) from (Raparthi et al., 2025) and Monte-Carlo (MC) family-kappa fits (with and without MAP (Maximum A Posteriori) regularization to prevent model overfitting) to quantify structural uncertainty in κ_{org}. The trained lab-derived κ_{org} models (the best-performing ones) were then transferred to ambient chemical composition at all measured diameters (i.e., 100, 150 nm, 200, and 250 nm), yielding time-resolved κ_{org} estimates, shown in Fig. 1. Ambient HTDMA or hygroscopicity measurements ($\kappa_{measured}$) were used to evaluate the classical ZSR κ_{chem} approach (mixing $\kappa_{org=0.1}$ with inorganic species) and develop a second-stage ML framework that predicts κ from the best-performing lab-derived κ_{org} predictor and the measured inorganic mass fractions. This ambient-trained ML approach empirically learns aerosol mixing behavior rather than assuming ideal internal mixing and provides ML-derived κ that reproduces $\kappa_{measured}$ more accurately than κ_{chem}, with consistently higher R^2 and lower RMSE and bias.

Machine learning techniques have recently been used to estimate aerosol hygroscopicity (Vu et al., 2021), where supervised regression techniques have generally been leveraged to implement the so-called proxies (Ferrer-Cid et al., 2024; Gupta et al., 2024). An ML-based proxy is an ML model that estimates a parameter using indirect measurements from other sensors. In this work, simple regression techniques are used to estimate aerosol hygroscopicity (κ) from 22 standard chemical compounds and ambient measurements. Specifically, the κ estimate $\hat{y}_t$ given some features x_t at a given time step t is set to:

$$\hat{y}_t \approx f_\kappa(x_t) \quad (5)$$

ML Function $f_\kappa(\cdot)$ uses the indirect measurements $x_t \subseteq \{x_{family\ groups}, x_{chem}\}$ such as family groups (i.e, Cx, CH, CHO) and chemical composition. To obtain the function $f_\kappa(\cdot)$, ML models from different families (linear, kernel, and ensemble) have been employed. Each model has its own hyperparameters, and identifying those that yield a good model is key. The data is randomly split into training and test sets, with 70% allocated to the training set and 30% to the test set. The training data is used to find the best hyperparameters and train the model. For each ML model, a grid search is performed on the training set using 5-fold cross-validation (CV) to optimize the model's hyperparameters, Θ. The following section describes the ML pipeline developed to design the hygroscopicity κ proxy.

2.4.1 Data processing and ML models

Four-machine learning (ML) models are tested and run to estimate hygroscopicity. RF and XGBoost outperform other models, including Monte Carlo and Multiple Linear Regression (MLR) with the Raparthi fitted technique (Raparthi et al., 2025) in terms of hygroscopicity. The comparative performance metrics (see Figs. S6-S7) indicate that RF achieved a superior correlation with $\kappa_{measured}$ across two sites for ambient measurements, underscoring its robustness in resolving differences across

https://doi.org/10.5194/egusphere-2026-1992
Preprint. Discussion started: 30 April 2026

various locations and compositional variability in aerosol hygroscopic estimates. All ML models were trained using standardized input features (z-scoring) and evaluated using repeated k-fold cross-validation (k = 5 folds × 10 repeats for κ_{org}; k = 10 for $\kappa_{measured}$). Hyperparameter optimization was performed via a randomized search for tree-based models (number of trees, depth, and learning rate for RF and XGB) and ridge regularization tuning for the linear models. To ensure the stability of predictions given the limited chemical diversity in the laboratory dataset, models were assessed for variance inflation, descriptor redundancy, and extrapolation behaviour when applied to ambient AMS compositions. Model interpretability was analyzed using permutation importance and Shapley additive explanation value diagnostics, confirming that oxygenation level (O:C), CHOgt, CH family groups, and inorganic fractions are the dominant drivers of κ_{org} and $\kappa_{measured}$, respectively (Fig. S9).

2.4.2 ML model validation

To find the optimal model for each data set and input variable, CV is performed. To validate the ML proxy for κ, a sensitivity analysis is performed using train-test splits (Random and temporal split for ambient measurements), in which models are tested across all possible combinations of input variables (chemical composition and families). Two different metrics are used to quantify the goodness of fit of the models: the coefficient of determination (R^2) and the root mean square error (RMSE), and independent consistency checks using Monte Carlo perturbations of the descriptor space.

$$\hat{y}_t \; or \; \kappa_{ML} \sim f\,(chem, families) \tag{6}$$

$$R^2(\boldsymbol{y}, \hat{\boldsymbol{y}}) = 1 - \frac{\sum_t (y_t - \hat{y}_t)^2}{\sum_t (y_t - \bar{y})^2}$$

$$RMSE(\boldsymbol{y}, \hat{\boldsymbol{y}}) = \sqrt{\frac{1}{T}\sum_t (y_t - \hat{y}_t)^2}$$

Where $\underline{y}$ denotes the average hygroscopicity value. The R^2 is defined as the proportion of variance explained by the model's output. The RMSE is defined as the root of the average square residuals.

These results are constrained by the size and chemical diversity of the laboratory compound set, which limits the representation of complex ambient organic mixtures. Moreover, applying lab-trained κ_{org} to ambient particles assumes that the laboratory descriptors remain chemically meaningful under atmospheric mixing, despite possible non-ideal or source-dependent effects.

2.4.3 Benefits and Limitations

Model validation strategies were selected according to the characteristics of the laboratory and ambient datasets. The laboratory dataset consisted of a relatively small number of compounds, limiting the feasibility of performing train-test splits without substantially reducing the available training data. Therefore, model robustness during the laboratory stage was evaluated using cross-validation and regularization techniques, such as maximum a posteriori (MAP) optimization, to stabilize parameter estimation. In contrast, the ambient dataset contained temporally resolved measurements, allowing more rigorous validation strategies. Both random train-test splitting and temporally structured splitting (time-blocked validation) were applied to evaluate model performance under different assumptions about temporal dependence. The random split provides a more conservative assessment of predictive skill by preventing information leakage across time periods, whereas a temporal split may be affected by compositional and site variability. Thus, the present framework should be interpreted as an informed and interpretable modelling approach. A possible limiting factor when applying to other datasets is the availability of the input family group from AMS. Understanding these can be essential for further steps in revising estimations of hygroscopicity parameterizations, and adding more organic compounds would improve the framework output. This framework enables the prediction of subsaturated aerosol growth over a wide particle-size range (100 to 250 nm), which directly controls aerosol optical properties and size distributions and, hence, aerosol-radiation interactions (Shen et al., 2021). Further establishes a quantitative link between laboratory-derived and ambient organic hygroscopicity, which gives information on climate-relevant aerosol behavior under subsaturated conditions.

https://doi.org/10.5194/egusphere-2026-1992
Preprint. Discussion started: 30 April 2026

3. Result

3.1 Measured Hygroscopic growth of organic compounds

Organic aerosols contribute 20% to 90% of the total fine particulate mass, but organic hygroscopicity remains poorly constrained due to their chemical complexity and limited size-resolved observations. To systematically investigate the influence of carbon number and functionalization on hygroscopicity, 22 representative organic compounds representing four family groups were selected and studied at 90 % relative humidity (Tables 1 and S1). The composition of organic aerosol is characterized through fragmentation patterns at specific mass-to-charge ratios (m/z) in AMS, from which elemental ratios (e.g., O:C and H:C) and oxidation proxies are derived, rather than explicit molecular identities (Canagaratna et al., 2007). These AMS-derived metrics are commonly interpreted using compositional families (e.g., C_x^+, $C_xH_y^+$, $C_xH_yO^+$, $C_xH_yO_{z>1}$) that reflect differences in functionalization and oxidation state. Using this conceptual framework, we relate laboratory-measured, size-segregated hygroscopicity of individual organic compounds to AMS-relevant compositional descriptors, providing a physically interpretable link between molecular-scale properties and bulk aerosol measurements.

The Carboxylic acids are the most abundant water-soluble components identified in atmospheric aerosols (Chebbi and Carlier, 1996; Mochida et al., 2003; Kundu et al., 2010). While the hygroscopic properties of straight-chain dicarboxylic acids have been extensively investigated in previous studies (Man et al., 2008; Kuwata et al., 2013; Rickards et al., 2013), size-resolved HTDMA measurements for dicarboxylic acids with additional substitutions and tricarboxylic acids are limited. To achieve an overview of the hygroscopicity of carboxylic acids, we measured the water uptake of several common straight-chain dicarboxylic acids in the atmosphere and further extended it to dicarboxylic acids with substitutions and tricarboxylic acids (Fig. 2). Among the straight-chain dicarboxylic acids, only malonic acid showed continuous hygroscopic growth with increasing diameter, and the measured GF at 90 % RH was 1.4 to 1.6 also agrees quite well with previous studies. Whereas the other dicarboxylic acids like Succinic, Pimelic, Adipic, and Suberic acid did not show any water uptake or growth at RH=90% for all diameters, maybe due to quite low solubility in water, and once crystallized, they would not deliquesce even under high-RH conditions (Peng et al., 2001; Peng and Chan, 2001; Man et al., 2008). It is worth noting that no previous data were available for suberic acid, except for those reported by (Han et al., 2022), which also aligns with our analysis. Although some slight variation is seen in family group fractions from AMS, and a very low change in GF (0.01-0.09) between diameters, a more or less the same family group fraction was seen for these hydrophobic dicarboxylic acids (Fig. 2). In contrast, maleic and tricarballylic acids show a sudden rise in growth for 150 nm although the family's fractions are same and other physical properties in measurements are too which is unexplainable and incomparable due to lack of size segregated previous data. We hypothesize that this change in maleic acid and tricarballylic acids is a size effect in DMA and possibly a change in the hygroscopicity of the organic compounds themselves. Similarly, this is also observed for levoglucosan and glucose (Fig. S1), while fructose and mannose show good agreement with previous measurements ((Han et al., 2022; Man et al., 2008); Figs. S1–S2).

Collectively, these results demonstrate that organic hygroscopicity cannot be described by a single compositional metric alone, motivating a multi-parameter framework that integrates size, functionalization, and physicochemical properties for improved parameterization of κ_{org}.

https://doi.org/10.5194/egusphere-2026-1992
Preprint. Discussion started: 30 April 2026

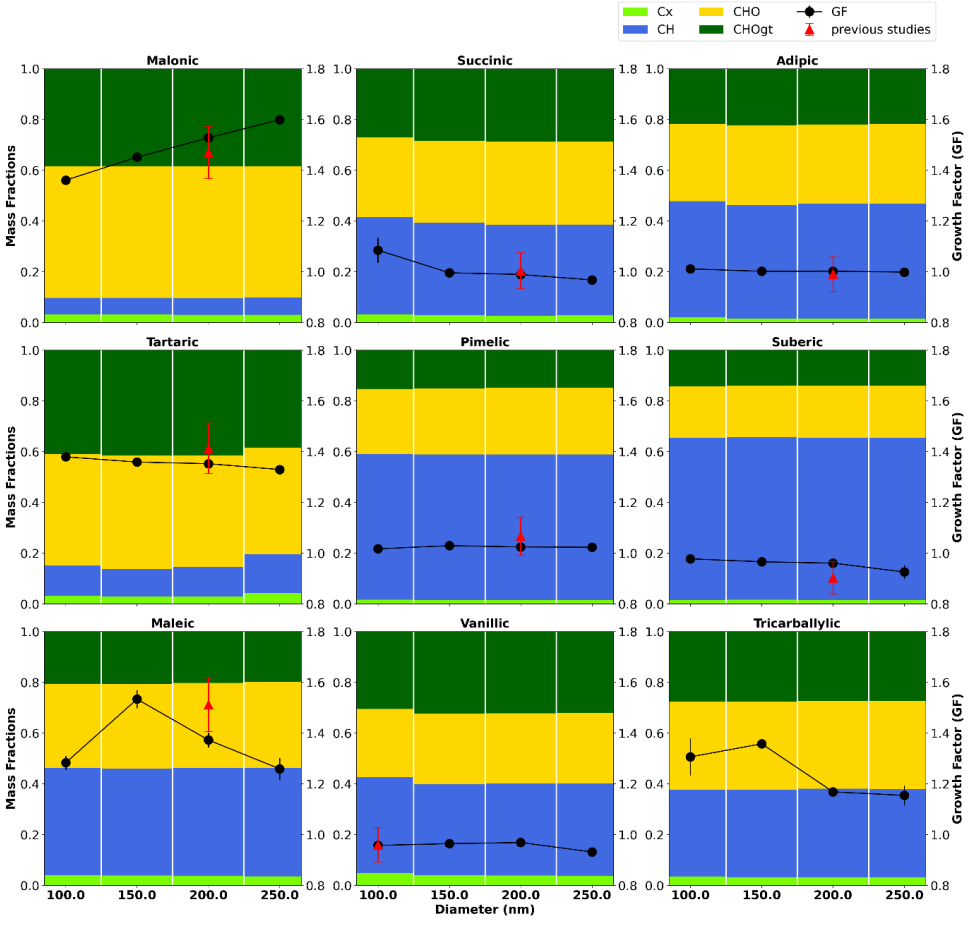

Figure 2: Size-segregated hygroscopicity (κ) of straight-chain dicarboxylic acid particles measured at 90 % RH, together with AMS-relevant compositional proxies expressed as family groups (C_x^+, $C_xH_y^+$, $C_xH_yO^+$, $C_xH_yO_{\geq 1}$, which also refer to CHOgt) for different particle diameters. Results are compared with available literature data to illustrate the influence of functionalization and particle size on organic hygroscopicity.

3.2 Hygroscopicity of organic compounds to their physicochemical properties

Converting measured growth factors to the hygroscopicity parameter κ using Eqs. (2) and (3) enable a consistent comparison of organic hygroscopic behaviour by explicitly accounting for water activity and thermodynamic constants. Figure S3 illustrates the size-resolved κ values for selected organic compounds and their dependence on molecular composition and oxidation-related ratios. The carboxylic acid group exhibits substantial variability in κ across compounds and particle diameters (Fig. S3a–e). For example, malonic acid exhibits a pronounced increase in κ with increasing diameter, from approximately 0.20 at 100 nm to approximately 0.35 at 250 nm, consistent with its high-water solubility. In contrast, succinic acid exhibits near-zero κ across all measured sizes, indicating limited water uptake under subsaturated conditions despite its similar carbon backbone. Tartaric acid displays moderate hygroscopicity with weaker size dependence, while maleic acid shows elevated κ at intermediate diameters, but reduced values at larger sizes, suggesting compound-specific interactions between molecular structure, solubility, and particle size. Tricarballylic acid exhibits a clear decrease in κ with increasing diameter, whereas levoglucosan shows consistently low hygroscopicity and a monotonic reduction in κ at larger sizes (Fig. 3f), consistent with previous observations of limited water uptake for saccharide-like compounds under subsaturated conditions. These results

https://doi.org/10.5194/egusphere-2026-1992
Preprint. Discussion started: 30 April 2026

demonstrate that even within a single functional class, κ_{org} can vary by more than an order of magnitude and exhibit distinct size dependencies, highlighting the limitations of assuming size-independence of κ for organic aerosols.

Figure S3g–i relates κ (measured at 200 nm) to oxidation proxies derived from AMS measurements, including O:C, CHO/CH, and CO_2/CH ratios. A general tendency of increasing κ with increasing O:C ratio is observed (Fig. S3g and Fig. S8), broadly consistent with previous laboratory and ambient studies (e.g., (Han et al., 2022)). More hygroscopic compounds, such as malonic and tartaric acids, occupy the higher O:C and higher κ regime, whereas weakly hygroscopic or hydrophobic compounds cluster at low O:C values. However, compounds with similar O:C ratios can differ substantially in κ, indicating that O:C alone is insufficient to constrain organic hygroscopicity uniquely (Petters et al., 2017). Such as, Xylithol and Meso-Erythritol have O:C of 0.6 but κ of 0.1 and 0.06, respectively (Fig. S3g), similarly Tartaric and Malonic acid have O:C of 1.5 with κ of 0.18 and 0.31, respectively, showing one is more hygroscopic and the other is less hygroscopic (Fig. S3).

Stronger separation among compounds is observed when κ is plotted against CHO/CH and CO_2/CH ratios (Fig. S3h–i). In particular, compounds with higher CHO/CH ratios tend to exhibit enhanced hygroscopicity, reflecting the increasing contribution of multifunctional oxygenated groups. The CO_2/CH ratio further highlights highly hygroscopic acids with multiple carboxyl groups, which show elevated κ despite overlapping O:C values with less hygroscopic compounds. These results suggest that ratios capturing functional group abundance and oxidation state provide additional explanatory power beyond bulk O:C alone. Consistent with (Peng et al., 2001; Han et al., 2022; Man et al., 2008), our results confirm that κ_{org} generally increases with oxidation level, and also reinforce that simplified proxies, such as O:C, introduce large uncertainties when applied to diverse organic mixtures. By resolving size-dependent κ and incorporating multiple oxidation-related ratios, this study demonstrates that organic hygroscopicity is governed by a combination of particle size, functionalization, and molecular structure rather than a single compositional metric. These findings motivate the inclusion of laboratory-constrained, multi-parameter descriptions of organic hygroscopicity in predictive frameworks and atmospheric models.

The observed compound-specific and size-dependent variability in κ, together with the non-unique relationships between κ and individual oxidation metrics (e.g., O:C and CO_2/CH), indicates that organic hygroscopicity cannot be reliably parameterized using single compositional descriptors. Although functional group classifications capture first-order trends, substantial scatter persists even among structurally similar compounds. This complexity motivates a multi-parameter, data-driven framework, which we address using a physically constrained machine-learning approach in the following section.

3.3 Laboratory analysis using Monte Carlo and Machine learning estimation of hygroscopicity

To evaluate the extent to which κ_{org} can be parameterized using compositional descriptors, we first implemented a Monte Carlo (MC)- based multilinear regression framework linking κ to organic family group properties and oxidation metrics. The MC approach allows systematic perturbation of input parameters and regression coefficients, thereby quantifying uncertainty and robustness in κ estimates derived from family-group-based descriptions. As shown in Fig. 3a, the MC ridge regression reproduces the first-order trends in measured κ but systematically underestimates hygroscopicity at higher κ values, exhibiting substantial scatter, particularly across different particle sizes. This behavior indicates that linear combinations of family-group proxies alone are insufficient to capture the full variability in size-resolved organic hygroscopicity. For comparison, κ was also estimated using the MLR proposed by Raparthi et al. (2025); $\kappa = 0.163\ (O/C) + 0.022\ C + 0.037\ O^* + 0.119$. Applying this equation to our laboratory dataset (Fig. 3b and S4) yields moderate agreement with the $\kappa_{measured}$, but shows pronounced deviations for several compounds and sizes, highlighting the limited transferability when applied outside the chemical space for which it was originally derived. In particular, the Raparthi MLR fails to capture size-dependent enhancements in κ and underperforms for compounds with similar oxidation metrics but differing functional-group distributions.

https://doi.org/10.5194/egusphere-2026-1992
Preprint. Discussion started: 30 April 2026

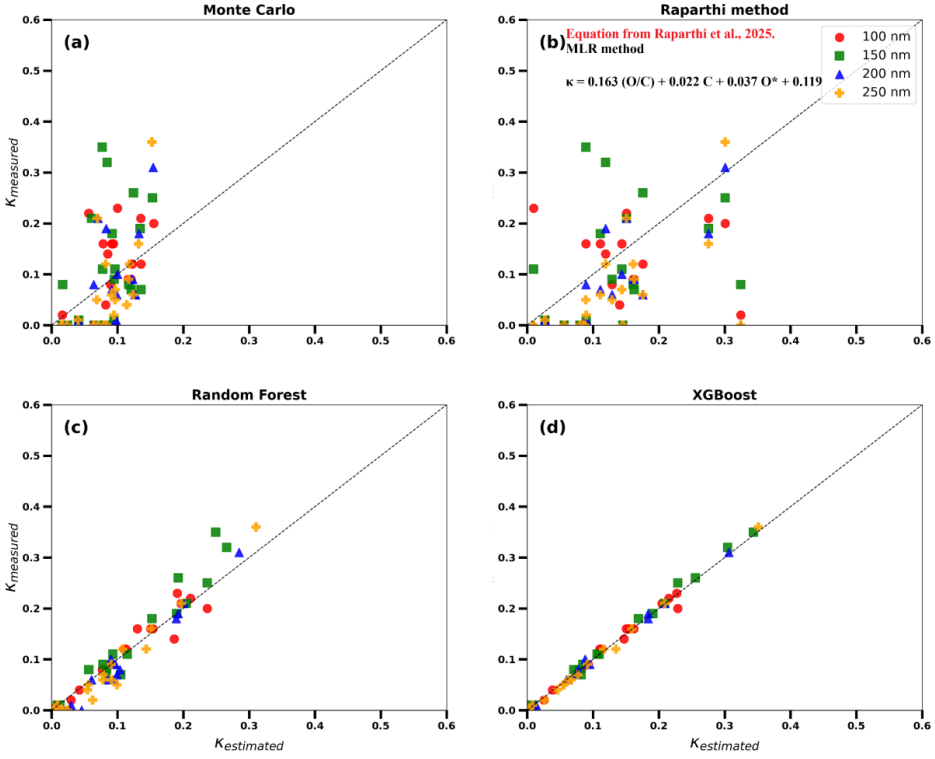

Figure 3: Comparison of measured size-resolved organic hygroscopicity (κ_{org}) for laboratory experiments with estimates derived from (a) Monte Carlo regression, (b) published (Raparthi et al., 2025) MLR, and two (c) & (d) machine-learning models. Nonlinear ML approaches, particularly XGBoost, capture size-dependent and functional-group-driven variability in κ that linear parameterizations cannot resolve.

To overcome these limitations, we implemented non-linear machine-learning models trained on the laboratory-derived, size-segregated κ dataset, incorporating family group descriptors, oxidation ratios, and particle size as simultaneous predictors. The random forest model (Fig. 3c) substantially improves agreement with measured κ, reducing scatter and capturing non-linear dependencies across functional groups. The gradient boosting (XGBoost) model (Fig. 3d) provides the best overall performance, yielding near one-to-one agreement across all particle sizes and chemical classes. These results demonstrate that κ_{org} is governed by coupled, non-linear interactions between molecular functionality and particle size that cannot be resolved by linear parameterizations alone. By integrating laboratory-constrained κ measurements with MC uncertainty analysis and machine-learning techniques, this framework provides a robust method for estimating κ_{org}, forming a strong basis for application to ambient aerosol measurements.

To assess atmospheric applicability, the laboratory-trained framework is applied to ambient aerosol data from Paris (2022 - ACROSS campaign) and Goldlauter, using family-group-resolved growth factors derived from AMS measurements. Further, the analysis can also be restricted to chemically stable periods, enabling a direct comparison between predicted and observed hygroscopicity.

3.4 Comparison with ambient measurement

We developed a two-stage workflow to translate laboratory-derived composition hygroscopicity relationships to ambient aerosol conditions, shown in Figs. 1 and 4a. In stage 1, laboratory HTDMA measurements were combined with family-group chemistry (Cx, CH, CHO, CHOgt) and O:C to infer physically plausible group κ parameters using constrained optimization with a Raparthi-based prior and uncertainty analysis (Monte Carlo/bootstrapping; Fig 1c), and further train supervised ML

https://doi.org/10.5194/egusphere-2026-1992
Preprint. Discussion started: 30 April 2026

models to predict κ_{org} from these descriptors (Fig. 1d). In stage 2, the lab-trained κ_{org} predictor was applied to size-resolved ambient family-group inputs and combined with AMS organic/inorganic partitioning to estimate κ and an organic scaling factor α under a bulk mixing constraint, enabling consistent reconstruction and evaluation of $\kappa_{estimate}$ against $\kappa_{measured}$ (from HTDMA; Fig 1e-g). Figure 4b-c shows that the temporal variability in family-group fractions is accompanied by corresponding variability in ML-estimated κ_{org}, Paris, and Goldlauter, respectively. In contrast, the ZSR reference assumes a constant $\kappa_{org = 0.1}$, providing only a baseline representation of the Paris site (Figs. 4b and S5). This assumption can bias hygroscopicity predictions when organic contributions dominate, as it does not capture the observed variability. The ML-derived κ_{org} reproduces these variations more realistically, particularly during periods of enhanced organic influence (pink-shaded regions; Fig. S6–S7), where the ZSR approach fails to represent the measured κ values. Similarly, this temporal variability in κ_{org} was observed for Goldlauter (Fig. 4c), though with less drastic fluctuations than in Paris, suggesting that ML captures this variation robustly in both cases, despite one being a more rural background and the other a suburban site.

The improved representation of κ variability, as reflected in the ML-derived κ_{org}, is also evident in the model validation results. Compared with the ZSR assumption of a constant $\kappa_{org = 0.1}$, the ML framework shows better agreement with $\kappa_{measured}$, suggesting that incorporating composition-dependent κ_{org} improves the prediction of aerosol hygroscopicity. This improvement highlights the importance of accounting for variability in organic hygroscopicity when evaluating κ in regions with substantial organic aerosol contributions. In continuation, the ML framework was evaluated against ambient hygroscopicity measurements using field data from Paris, France (June–July 2022) and Goldlauter, Germany (September-October 2010). Figure 5 demonstrates that simple mixing-rule approaches (ZSR) and multilinear regression (MLR) exhibit weak agreement with measured κ ($R^2 \approx$ 0.1–0.2), substantially underestimating both the variability and magnitude of ambient hygroscopicity. In contrast, non-linear machine-learning models (Random Forest and XGBoost) reproduce $\kappa_{measured}$ with high correlation for both 100 and 200 nm particles ($R^2 \approx$ 0.92–0.96; Paris; Fig 5c-d), indicating that ambient hygroscopicity cannot be adequately described using linearized composition-κ relationships. A similar pattern of estimation and improvement was observed for Goldlauter ($R^2 \approx$ 0.92–0.94; Fig 5h-i). The temporal evolution of κ further highlights the robustness of the ML approach and closely tracks measured short-term variability and multi-day trends across both datasets; in contrast, ZSR-based estimates systematically diminish the variability effect (Fig. 5e and 5j). The strong agreement across two independent campaigns and size ranges demonstrates that the ML framework captures effective mixing behaviour under real atmospheric conditions, including partial external mixing and non-ideal interactions of organics that are not represented in classical ZSR formulations.

Training ML models directly on ambient AMS (including Cx, CH, CHO, CHOgt, and inorganic fractions) composition and $\kappa_{measured}$ (by HTDMA) allows the model to learn effective hygroscopic behavior without imposing internal mixture assumptions. Incorporating laboratory-trained κ_{org} into ambient ML models, together with inorganic fractions, further constrains predictions while retaining real-world mixing behavior. This hybrid approach bridges the understanding of laboratory processes and ambient complexity while preserving physical interpretability. ZSR is retained solely for baseline comparison; validation and interpretation should rely on ML-predicted κ, which provides a more accurate representation of ambient aerosol behaviour.

https://doi.org/10.5194/egusphere-2026-1992
Preprint. Discussion started: 30 April 2026

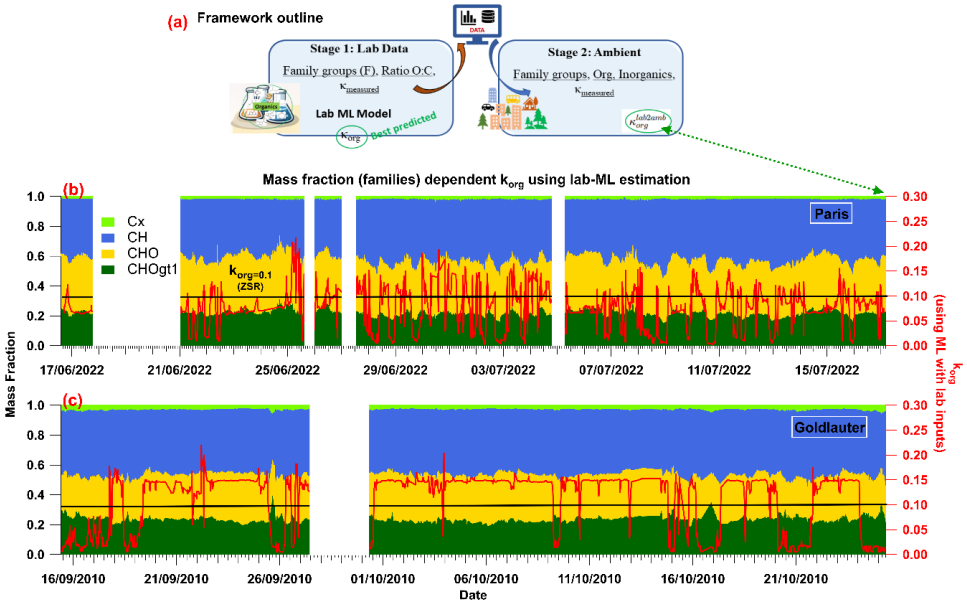

425 **Figure 4: (a) Two-stage lab-to-ambient framework for estimating organic hygroscopicity (κ_{org}) from family-group chemistry and its application to ambient aerosol. (b-c) Time series of family-group mass fractions (left axis) and lab-ML-derived κ_{org} (right axis) for Paris and Goldlauter, with the ZSR reference (κ_{org} = 0.1) shown for comparison, also detailed in Figs. S6-7.**

To assess the influence of laboratory-derived κ_{org} on ambient aerosol hygroscopicity predictions, we compared Random Forest (RF) model outputs from an ambient-only framework (ML model trained and tested only on site-specific chemical
430 composition) with our ML approach that incorporates κ_{org} derived from laboratory measurements. The evaluation was performed for two contrasting European environments, Paris (suburban) and Goldlauter (rural background), using independent ambient datasets. Figures 6a and 6c show RF model predictions without κ_{org} input, where κ was estimated using bulk chemical composition (organic and inorganic fractions), black carbon, and size distribution. Under these conditions, the model captures the general variability in κ but shows increased scatter, particularly at intermediate values of κ. The resulting coefficients of
435 determination are R^2 = 0.82 for Paris and R^2 = 0.60 for Goldlauter, indicating reduced predictive skill, especially at the rural site where organic aerosol composition dominates. When κ_{org} derived from laboratory inputs is included as an additional predictor (Figures 6b and 6d), model performance improves at both sites. The RF predictions align closely with the 1:1 line, yielding R^2 values of 0.96 for Paris and 0.94 for Goldlauter. This improvement is consistent across all particle sizes (i.e., 100 nm and 200 nm; Fig. 6), indicating that the laboratory-informed κ_{org} captures size-dependent organic hygroscopicity that is not
440 fully captured by bulk composition alone.

https://doi.org/10.5194/egusphere-2026-1992
Preprint. Discussion started: 30 April 2026

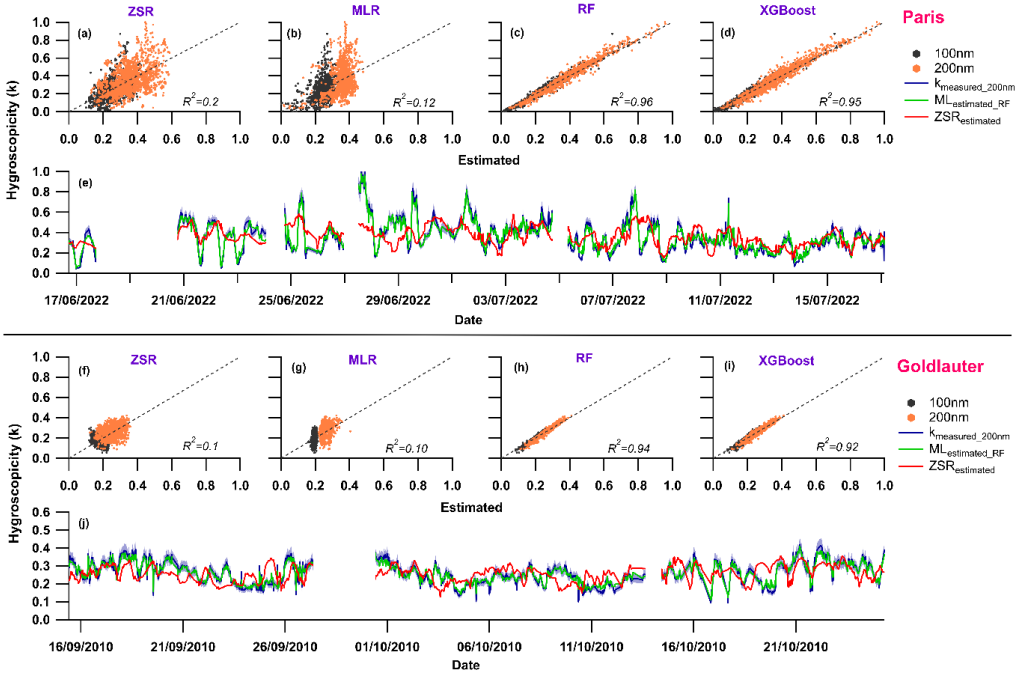

Figure 5: Comparison of hygroscopicity estimation for different approaches with $\kappa_{measured}$. (a-e) The estimates of κ are shown alongside $\kappa_{measured}$ in a scatterplot and timeseries, where ML approaches such as MLR, RF, and XGBoost are used to pre-test laboratory-standard organic compounds using family-group kappa classifications, and the ZSR approach mixes $\kappa_{org=0.1}$ with inorganic species for Paris. (f-j) Similar comparison and analysis are presented for Goldlauter.

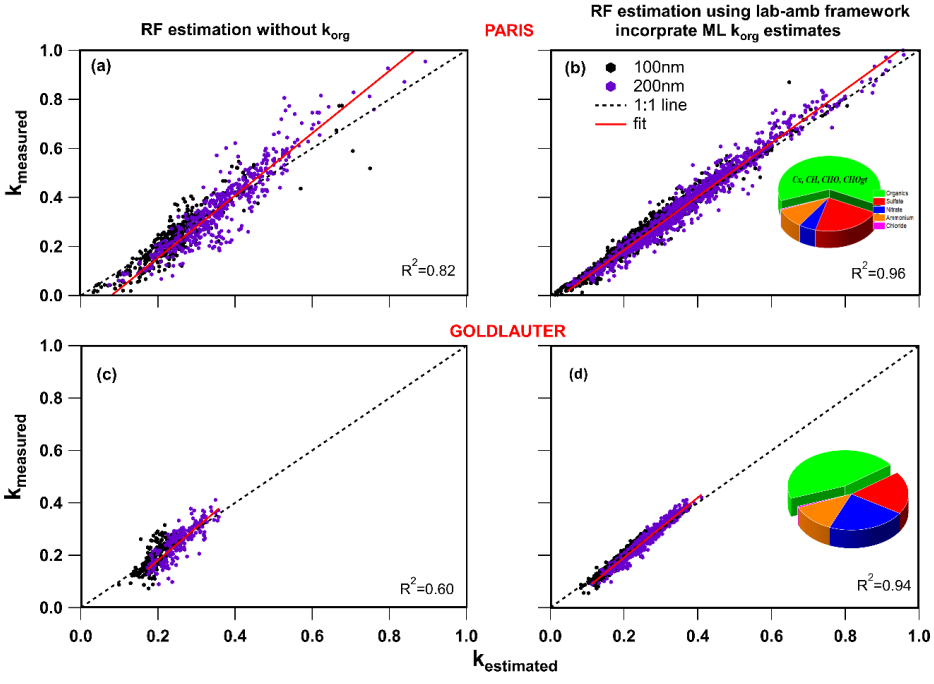

Figure 6: Comparison of the Random Forest (RF) model performance for estimating κ at Paris and Goldlauter with and without laboratory-derived κ_{org} input. (a & c) Show RF-estimated κ versus measured κ for Paris and Goldlauter, respectively, using ambient inputs only, including chemical composition (organics and inorganics + BC). (b & d) Show corresponding RF estimations after

https://doi.org/10.5194/egusphere-2026-1992
Preprint. Discussion started: 30 April 2026

incorporating κ_{org} derived from laboratory analysis and ambient (organics (Cx, CH, CHO, CHOgt) + inorganic) as additional features, showing that the high contribution of organics plays an important role. Data points are color-coded by particle diameter (100 nm and 200 nm). Inclusion of κ_{org} substantially improves model performance, increasing the coefficient of determination from 0.82 to 0.96 for Paris and from 0.60 to 0.94 for Goldlauter, demonstrating the added predictive value of laboratory-constrained organic hygroscopicity in ambient ML applications.

The enhanced performance demonstrates that incorporating physically constrained laboratory measurements into ML frameworks significantly reduces uncertainty in ambient κ predictions. In particular, the significant improvement observed at Goldlauter underscores the importance of addressing organic hygroscopicity in environments with complex, variable organic aerosol sources. Although these cases were of a dominant organic contribution (50-62% organic fraction) at the sites, if inorganic components, such as sulphuric acids or sea spray, are dominant or account for more than 70-80% of the fraction, the organic role is probably negligible. These results highlight the importance of integrating controlled laboratory studies with data-driven ambient models to enhance the representation of aerosol hygroscopicity in atmospheric applications.

4. Conclusion

In this study, we developed a laboratory-anchored, machine-learning framework to quantitatively link organic aerosol hygroscopicity from single-compound measurements to ambient aerosol κ. By organizing individual organic species into functional family groups with characteristic hygroscopic properties, we establish a physically interpretable basis for representing the organic fraction of atmospheric aerosol. By measuring the hygroscopic growth of 22 atmospherically relevant organic compounds-including carboxylic acids, amino acids, sugars, and alcohols—across the submicrometer size range using HTDMA, we provide a detailed laboratory basis for understanding how molecular structure and functionalization control organic hygroscopicity. The results demonstrate that κ_{org} varies strongly with particle size, functional groups, and molecular interactions, with increased functionalization generally enhancing water uptake and inducing pronounced size dependence. The observed diversity in hygroscopic behavior among structurally similar compounds further highlights the limitations of simplified oxidation-based or single-parameter κ representations.

These findings underscore the need for data-driven frameworks that can integrate this molecular complexity into descriptions of ambient aerosols. While functional-group-based classifications provide a useful first-order approximation, they alone cannot capture the non-unique and nonlinear relationships between chemical composition and hygroscopicity. By leveraging laboratory-constrained κ_{org} values for organic families, we developed a physically informed machine-learning framework that maps molecular-scale hygroscopicity to ambient aerosol observations. Application of this hybrid approach to urban and rural environments leads to substantial improvements in predicting ambient κ, increasing the coefficient of determination from 0.82 to 0.96 in Paris and from 0.60 to 0.94 in Goldlauter compared to conventional composition-based parameterizations. The framework enables the prediction of subsaturated aerosol growth over a wide particle size range, which directly controls aerosol optical properties and size distributions, and hence aerosol–radiation interactions and radiative forcing, and extends to cloud droplet activation. This establishes a quantitative link between laboratory-derived organic hygroscopicity and climate-relevant aerosol behavior under both subsaturated and supersaturated conditions. Although a possible limiting factor when applying to other datasets is the availability of family groups from AMS, further, it is more suitable when the organic fraction contributes largely; it remains relevant even in an inorganic-dominated environment. Understanding these can be essential for subsequent steps in revising estimations of hygroscopicity parameterizations, and adding more organic compounds to laboratory studies would improve the framework's output.

A key strength of the presented approach is its modular and community-oriented design. The laboratory-derived κ_{org} database, machine-learning tools, and processing workflows are made available to the community, enabling application to additional regions and atmospheric regimes. As new laboratory measurements become available, additional organic compound classes can be incorporated without empirical recalibration to ambient data, allowing the framework to evolve alongside advances in laboratory aerosol chemistry. Together, this work provides a scalable, physically grounded pathway from molecular-scale

https://doi.org/10.5194/egusphere-2026-1992
Preprint. Discussion started: 30 April 2026

organic composition to predictions of aerosol growth, cloud interactions, and radiative forcing, offering a systematic route to reducing major uncertainties in atmospheric and climate modeling.

Code availability

The code and other processing toolkits can be made available upon request to the first author (deshmukh@tropos.de). ML output figure codes are available in the Figshare repository and via the referenced DOI (Deshmukh, 2026).

Data availability

Level 3 datasets from the ACROSS field campaign for the SIRTA site used in the present study are available on the AERIS data center and referenced by DOI. Also, data are available upon request to the author (deshmukh@tropos.de). ML output results are available in the Figshare repository and via the referenced DOI (Deshmukh, 2026).

Author contribution

SD performed the formal analysis and wrote the original draft. SD and LP performed the investigation and data curation. SD and LP contributed to the experimental setup and operation of the instrumentation, as well as the data collection and analysis. SD, LP, MP, and SH provided the methodology and conceptualisation. MP and HH provided supervision and validation. LP, SH, BW, HH, and MP contributed to the review and editing of the manuscript. All authors commented and contributed.

Competing interests

One co-author (B. Wehner) is a member of the editorial board for the Journal of ACP. The contact author has declared that none of the other authors has any competing interests.

Disclaimer

Publisher's note: Copernicus Publications remains neutral concerning jurisdictional claims in published maps and institutional affiliations.

Funding

This work has been supported by the DFG H-AMS project (reference WE 2757/4-1) and is also involved in the ACROSS campaign. The ACROSS project has received funding from the French National Research Agency 475 (ANR) under the investment program integrated into France 2030, with the reference ANR−17−MPGA−0002, and it was supported by the French National program LEFE (Les Enveloppes Fluides et 610 l'Environnement) of the CNRS−INSU (Centre National de la Recherche Scientifique/Institut National des Sciences de l'Univers).

Acknowledgements

We acknowledge support from the SIRTA facility in conducting measurements and collaboration. We appreciate the support from other groups involved in measurement with us, including LSCE (Laboratoire des Sciences du Climat et de l'Environnement), LAMP (Laboratoire de Météorologie Physique), and members of the Institut National de l'Environnement Industriel et des Risques. I want to acknowledge support from TROPOS, the University of Leipzig, and my PhD colleagues.

https://doi.org/10.5194/egusphere-2026-1992
Preprint. Discussion started: 30 April 2026

References

Aiken, A. C., Decarlo, P. F., Kroll, J. H., Worsnop, D. R., Huffman, J. A., Docherty, K. S., Ulbrich, I. M., Mohr, C., Kimmel, J. R., Sueper, D., Sun, Y., Zhang, Q., Trimborn, A., Northway, M., Ziemann, P. J., Canagaratna, M. R., Onasch, T. B., Alfarra, M. R., Prevot, A. S. H., Dommen, J., Duplissy, J., Metzger, A., Baltensperger, U., and Jimenez, J. L.: O/C and OM/OC ratios of primary, secondary, and ambient organic aerosols with high-resolution time-of-flight aerosol mass spectrometry, Environ. Sci. Technol., 42, 4478–4485, https://doi.org/10.1021/ES703009Q/SUPPL_FILE/ES703009Q-FILE002.PDF, 2008.

Alfarra, M. R., Paulsen, D., Gysel, M., Garforth, A. A., Dommen, J., Prévôt, A. S. H., Worsnop, D. R., Baltensperger, U., and Coe, H.: A mass spectrometric study of secondary organic aerosols formed from the photooxidation of anthropogenic and biogenic precursors in a reaction chamber, Atmos. Chem. Phys., 6, 5279–5293, https://doi.org/10.5194/ACP-6-5279-2006, 2006.

AR5 Climate Change 2013: The Physical Science Basis — IPCC: https://www.ipcc.ch/report/ar5/wg1/, last access: 31 August 2024.

Description – across: https://across.aeris-data.fr/description/, last access: 24 September 2024.

Bezantakos, S., Barmpounis, K., Giamarelou, M., Bossioli, E., Tombrou, M., Mihalopoulos, N., Eleftheriadis, K., Kalogiros, J., Allan, J. D., Bacak, A., Percival, C. J., Coe, H., and Biskos, G.: Chemical composition and hygroscopic properties of aerosol particles over the Aegean Sea, Atmos. Chem. Phys., 13, 11595–11608, https://doi.org/10.5194/ACP-13-11595-2013, 2013.

Bordoni, S., Kang, S. M., Shaw, T. A., Simpson, I. R., and Zanna, L.: The futures of climate modeling, npj Climate and Atmospheric Science 2025 8:1, 8, 1–6, https://doi.org/10.1038/s41612-025-00955-8, 2025.

Canagaratna, M. R., Jayne, J. T., Jimenez, J. L., Allan, J. D., Alfarra, M. R., Zhang, Q., Onasch, T. B., Drewnick, F., Coe, H., Middlebrook, A., Delia, A., Williams, L. R., Trimborn, A. M., Northway, M. J., DeCarlo, P. F., Kolb, C. E., Davidovits, P., and Worsnop, D. R.: Chemical and microphysical characterization of ambient aerosols with the aerodyne aerosol mass spectrometer, Mass Spectrom. Rev., 26, 185–222, https://doi.org/10.1002/MAS.20115, 2007.

Canagaratna, M. R., Jimenez, J. L., Kroll, J. H., Chen, Q., Kessler, S. H., Massoli, P., Hildebrandt Ruiz, L., Fortner, E., Williams, L. R., Wilson, K. R., Surratt, J. D., Donahue, N. M., Jayne, J. T., and Worsnop, D. R.: Elemental ratio measurements of organic compounds using aerosol mass spectrometry: Characterization, improved calibration, and implications, Atmos. Chem. Phys., 15, 253–272, https://doi.org/10.5194/ACP-15-253-2015, 2015.

Chan, M. N. and Chan, C. K.: Mass transfer effects in hygroscopic measurements of aerosol particles, Atmos. Chem. Phys, 2703–2712 pp., https://doi.org/doi.org/10.5194/acp-5-2703-2005, 2005.

Chebbi, A. and Carlier, P.: Carboxylic acids in the troposphere, occurrence, sources, and sinks: A review, Atmos. Environ., 30, 4233–4249, https://doi.org/10.1016/1352-2310(96)00102-1, 1996.

Chen, Y., Haywood, J., Wang, Y., Malavelle, F., Jordan, G., Partridge, D., Fieldsend, J., De Leeuw, J., Schmidt, A., Cho, N., Oreopoulos, L., Platnick, S., Grosvenor, D., Field, P., and Lohmann, U.: Machine learning reveals climate forcing from aerosols is dominated by increased cloud cover, Nature Geoscience 2022 15:8, 15, 609–614, https://doi.org/10.1038/s41561-022-00991-6, 2022.

DeCarlo, P. F., Kimmel, J. R., Trimborn, A., Northway, M. J., Jayne, J. T., Aiken, A. C., Gonin, M., Fuhrer, K., Horvath, T., Docherty, K. S., Worsnop, D. R., and Jimenez, J. L.: Field-deployable, high-resolution, time-of-flight aerosol mass spectrometer, Anal. Chem., 78, 8281–8289, https://doi.org/10.1021/AC061249N/SUPPL_FILE/AC061249NSI20060905_075156.PDF, 2006.

Deshmukh, S., Poulain, L., Wehner, B., Henning, S., Petit, J.-E., Fombelle, P., Favez, O., Herrmann, H., and Pöhlker, M.: External particle mixing influences hygroscopicity in a sub-urban area, Atmos. Chem. Phys., 25, 741–758, https://doi.org/10.5194/acp-25-741-2025, 2025.

Deshmukh, S.: Dataset for Machine learning output: From single compound to ambient aerosols., https://doi.org/10.6084/m9.figshare.31953339, 2026.

https://doi.org/10.5194/egusphere-2026-1992
Preprint. Discussion started: 30 April 2026

Dinar, E., Mentel, T. F., and Rudich, Y.: The density of humic acids and humic like substances (HULIS) from fresh and aged wood burning and pollution aerosol particles, Atmos. Chem. Phys., 6, 5213–5224, https://doi.org/10.5194/ACP-6-5213-2006, 2006.

Duplissy, J., Gysel, M., Sjogren, S., Meyer, N., Good, N., Kammermann, L., Michaud, V., Weigel, R., Martins Dos Santos, S., Gruening, C., Villani, P., Laj, P., Sellegri, K., Metzger, A., McFiggans, G. B., Wehrle, G., Richter, R., Dommen, J., Ristovski, Z., Baltensperger, U., and Weingartner, E.: Intercomparison study of six HTDMAs: Results and recommendations, Atmos. Meas. Tech., 2, 363–378, https://doi.org/10.5194/AMT-2-363-2009, 2009.

Estillore, A. D., Hettiyadura, A. P. S., Qin, Z., Leckrone, E., Wombacher, B., Humphry, T., Stone, E. A., and Grassian, V. H.: Water Uptake and Hygroscopic Growth of Organosulfate Aerosol, Environ. Sci. Technol., 50, 4259–4268, https://doi.org/10.1021/ACS.EST.5B05014, 2016.

Ferrer-Cid, P., Paredes-Ahumada, J. A., Allka, X., Guerrero-Zapata, M., Barcelo-Ordinas, J. M., and Garcia-Vidal, J.: A Data-Driven Framework for Air Quality Sensor Networks, IEEE Internet of Things Magazine, 7, 128–134, https://doi.org/10.1109/IOTM.001.2300112, 2024.

Gupta, P., Ferrer-Cid, P., Barcelo-Ordinas, J. M., Garcia-Vidal, J., Soni, V. K., Pöhlker, M. L., Ahlawat, A., and Viana, M.: Estimating black carbon levels using machine learning models in high-concentration regions, Science of The Total Environment, 948, 174804, https://doi.org/10.1016/J.SCITOTENV.2024.174804, 2024.

Gysel, M., Crosier, J., Topping, D. O., Whitehead, J. D., Bower, K. N., Cubison, M. J., Williams, P. I., Flynn, M. J., McFiggans, G. B., and Coe, H.: Closure study between chemical composition and hygroscopic growth of aerosol particles during TORCH2, Atmos. Chem. Phys., 7, https://doi.org/10.5194/acp-7-6131-2007, 2007.

Gysel, M., McFiggans, G. B., and Coe, H.: Inversion of tandem differential mobility analyser (TDMA) measurements, J. Aerosol Sci., 40, 134–151, https://doi.org/10.1016/j.jaerosci.2008.07.013, 2009.

Gysel, M., Laborde, M., Olfert, J. S., Subramanian, R., and Gréhn, A. J.: Effective density of Aquadag and fullerene soot black carbon reference materials used for SP2 calibration, Atmos. Meas. Tech., 4, 2851–2858, https://doi.org/10.5194/AMT-4-2851-2011, 2011.

Haeffelin, M., Barthès, L., Bock, O., Boitel, C., Bony, S., Bouniol, D., Chepfer, H., Chiriaco, M., Cuesta, J., Delanoë, J., Drobinski, P., Dufresne, J.-L., Flamant, C., Grall, M., Hodzic, A., Hourdin, F., Lapouge, F., Lemaˆıtre, Y. L., Mathieu, A., Morille, Y., Naud, C., Noël, V., O'hirok, W., Pelon, J., Pietras, C., Protat, A., Romand, B., Scialom, G., and Vautard, R.: Annales Geophysicae SIRTA, a ground-based atmospheric observatory for cloud and aerosol research, 23, 253–275, 2005.

Han, S., Hong, J., Luo, Q., Xu, H., Tan, H., Wang, Q., Tao, J., Zhou, Y., Peng, L., He, Y., Shi, J., Ma, N., Cheng, Y., and Su, H.: Hygroscopicity of organic compounds as a function of organic functionality, water solubility, molecular weight, and oxidation level, Atmos. Chem. Phys., 22, 3985–4004, https://doi.org/10.5194/acp-22-3985-2022, 2022.

Jiang, Y., Ma, Y., Zheng, J., Ye, N., and Yuan, C.: Characterization of size-resolved aerosol hygroscopicity and liquid water content in Nanjing of the Yangtze River Delta, Journal of Environmental Sciences, 151, 26–41, https://doi.org/10.1016/J.JES.2024.03.035, 2025.

Jimenez, J. L., Canagaratna, M. R., Donahue, N. M., Prevot, A. S. H., Zhang, Q., Kroll, J. H., DeCarlo, P. F., Allan, J. D., Coe, H., Ng, N. L., Aiken, A. C., Docherty, K. S., Ulbrich, I. M., Grieshop, A. P., Robinson, A. L., Duplissy, J., Smith, J. D., Wilson, K. R., Lanz, V. A., Hueglin, C., Sun, Y. L., Tian, J., Laaksonen, A., Raatikainen, T., Rautiainen, J., Vaattovaara, P., Ehn, M., Kulmala, M., Tomlinson, J. M., Collins, D. R., Cubison, M. J., Dunlea, E. J., Huffman, J. A., Onasch, T. B., Alfarra, M. R., Williams, P. I., Bower, K., Kondo, Y., Schneider, J., Drewnick, F., Borrmann, S., Weimer, S., Demerjian, K., Salcedo, D., Cottrell, L., Griffin, R., Takami, A., Miyoshi, T., Hatakeyama, S., Shimono, A., Sun, J. Y., Zhang, Y. M., Dzepina, K., Kimmel, J. R., Sueper, D., Jayne, J. T., Herndon, S. C., Trimborn, A. M., Williams, L. R., Wood, E. C., Middlebrook, A. M., Kolb, C. E., Baltensperger, U., and Worsnop, D. R.: Evolution of organic aerosols in the atmosphere, Science, 326, 1525–1529, https://doi.org/10.1126/SCIENCE.1180353, 2009.

https://doi.org/10.5194/egusphere-2026-1992
Preprint. Discussion started: 30 April 2026

Kondo, Y., Sahu, L., Moteki, N., Khan, F., Takegawa, N., Liu, X., Koike, M., and Miyakawa, T.: Consistency and Traceability of Black Carbon Measurements Made by Laser-Induced Incandescence, Thermal-Optical Transmittance, and Filter-Based Photo-Absorption Techniques, Aerosol Science and Technology, 45, 295–312, https://doi.org/10.1080/02786826.2010.533215, 2011.

Kundu, S., Kawamura, K., Andreae, T. W., Hoffer, A., and Andreae, M. O.: Molecular distributions of dicarboxylic acids, ketocarboxylic acids and α-dicarbonyls in biomass burning aerosols: Implications for photochemical production and degradation in smoke layers, Atmos. Chem. Phys., 10, 2209–2225, https://doi.org/10.5194/ACP-10-2209-2010, 2010.

Kuwata, M., Shao, W., Lebouteiller, R., and Martin, S. T.: Classifying organic materials by oxygen-to-carbon elemental ratio to predict the activation regime of Cloud Condensation Nuclei (CCN), Atmos. Chem. Phys., 13, 5309–5324, https://doi.org/10.5194/ACP-13-5309-2013, 2013.

Laj, P., Myhre, C. L., Riffault, V., Amiridis, V., Fuchs, H., Eleftheriadis, K., Petäjä, T., Salameh, T., Kivekäs, N., Juurola, E., Saponaro, G., Philippin, S., Cornacchia, C., Arboledas, L. A., Baars, H., Claude, A., De Mazière, M., Dils, B., Dufresne, M., Evangeliou, N., Favez, O., Fiebig, M., Haeffelin, M., Herrmann, H., Höhler, K., Illmann, N., Kreuter, A., Ludewig, E., Marinou, E., Möhler, O., Mona, L., Murberg, L. E., Nicolae, D., Novelli, A., O'Connor, E., Ohneiser, K., Altieri, R. M. P., Picquet-Varrault, B., van Pinxteren, D., Pospichal, B., Putaud, J. P., Reimann, S., Siomos, N., Stachlewska, I., Tillmann, R., Voudouri, K. A., Wandinger, U., Wiedensohler, A., Apituley, A., Comerón, A., Gysel-Beer, M., Mihalopoulos, N., Nikolova, N., Pietruczuk, A., Sauvage, S., Sciare, J., Skov, H., Svendby, T., Swietlicki, E., Tonev, D., Vaughan, G., Zdimal, V., Baltensperger, U., Doussin, J. F., Kulmala, M., Pappalardo, G., Sundet, S. S., and Vana, M.: Aerosol, Clouds and Trace Gases Research Infrastructure (ACTRIS): The European Research Infrastructure Supporting Atmospheric Science, Bull. Am. Meteorol. Soc., 105, E1098–E1136, https://doi.org/10.1175/BAMS-D-23-0064.1, 2024.

Li, J., Carlson, B. E., Yung, Y. L., Lv, D., Hansen, J., Penner, J. E., Liao, H., Ramaswamy, V., Kahn, R. A., Zhang, P., Dubovik, O., Ding, A., Lacis, A. A., Zhang, L., and Dong, Y.: Scattering and absorbing aerosols in the climate system, Nature Reviews Earth & Environment 2022 3:6, 3, 363–379, https://doi.org/10.1038/s43017-022-00296-7, 2022.

Li, Z., Lau, W. K. M., Ramanathan, V., Wu, G., Ding, Y., Manoj, M. G., Liu, J., Qian, Y., Li, J., Zhou, T., Fan, J., Rosenfeld, D., Ming, Y., Wang, Y., Huang, J., Wang, B., Xu, X., Lee, S. S., Cribb, M., Zhang, F., Yang, X., Zhao, C., Takemura, T., Wang, K., Xia, X., Yin, Y., Zhang, H., Guo, J., Zhai, P. M., Sugimoto, N., Babu, S. S., and Brasseur, G. P.: Aerosol and monsoon climate interactions over Asia, Reviews of Geophysics, 54, 866–929, https://doi.org/10.1002/2015RG000500, 2016.

Man, N. C., Kreidenweis, S. M., and Chan, C. K.: Measurements of the Hygroscopic and Deliquescence Properties of Organic Compounds of Different Solubilities in Water and Their Relationship with Cloud Condensation Nuclei Activities, Environ. Sci. Technol., 42, 3602–3608, https://doi.org/10.1021/ES7023252, 2008.

Massling, A., Leinert, S., Wiedensohler, A., and Covert, D.: Hygroscopic growth of sub-micrometer and one-micrometer aerosol particles measured during ACE-Asia, Atmos. Chem. Phys, 3249–3259 pp., 2007.

Mochida, M., Kawabata, A., Kawamura, K., Hatsushika, H., and Yamazaki, K.: Seasonal variation and origins of dicarboxylic acids in the marine atmosphere over the western North Pacific, Journal of Geophysical Research: Atmospheres, 108, https://doi.org/10.1029/2002JD002355;WGROUP:STRING:PUBLICATION, 2003.

Nakao, S.: Why would apparent κ linearly change with O/C? Assessing the role of volatility, solubility, and surface activity of organic aerosols, Aerosol Science and Technology, 51, 1377–1388, https://doi.org/10.1080/02786826.2017.1352082;CTYPE:STRING:JOURNAL, 2017.

Park, K., Kittelson, D. B., Zachariah, M. R., and McMurry, P. H.: Measurement of inherent material density of nanoparticle agglomerates, Journal of Nanoparticle Research, 6, 267–272, https://doi.org/10.1023/B:NANO.0000034657.71309.E6/METRICS, 2004.

Peng, C. and Chan, C. K.: The water cycles of water-soluble organic salts of atmospheric importance, Atmos. Environ., 35, 1183–1192, https://doi.org/10.1016/S1352-2310(00)00426-X, 2001.

https://doi.org/10.5194/egusphere-2026-1992
Preprint. Discussion started: 30 April 2026

Peng, C., Chan, M. N., and Chan, C. K.: The Hygroscopic Properties of Dicarboxylic and Multifunctional Acids: Measurements and UNIFAC Predictions, Environ. Sci. Technol., 35, 4495–4501, https://doi.org/10.1021/ES0107531, 2001.

Petit, J.-E., Favez, O., Sciare, J., Crenn, V., Sarda-Estève, R., Bonnaire, N., Močnik, G., Dupont, J.-C., Haeffelin, M., and Leoz-Garziandia, E.: Two years of near real-time chemical composition of submicron aerosols in the region of Paris using an Aerosol Chemical Speciation Monitor (ACSM) and a multi-wavelength Aethalometer, Atmos. Chem. Phys, 15, 2985–3005, https://doi.org/10.5194/acp-15-2985-2015, 2015.

Petters, M. D. and Kreidenweis, S. M.: A single parameter representation of hygroscopic growth and cloud condensation nucleus activity, Atmos. Chem. Phys., 7, 1961–1971, https://doi.org/10.5194/ACP-7-1961-2007, 2007.

Petters, M. D., Wex, H., Carrico, C. M., Hallbauer, E., Massling, A., McMeeking, G. R., Poulain, L., Wu, Z., Kreidenweis, S. M., and Stratmann, F.: Towards closing the gap between hygroscopic growth and activation for secondary organic aerosol-Part 2: Theoretical approaches, Atmos. Chem. Phys., 9, 3999–4009, https://doi.org/10.5194/ACP-9-3999-2009, 2009.

Petters, S. S., Pagonis, D., Claflin, M. S., Levin, E. J. T., Petters, M. D., Ziemann, P. J., and Kreidenweis, S. M.: Hygroscopicity of Organic Compounds as a Function of Carbon Chain Length and Carboxyl, Hydroperoxy, and Carbonyl Functional Groups, Journal of Physical Chemistry A, 121, 5164–5174, https://doi.org/10.1021/acs.jpca.7b04114, 2017.

Raparthi, N., Wexler, A. S., and Dillner, A. M.: Hygroscopicity of Organic Compounds as a Function of Their Physicochemical Properties, ACS ES&T Air, https://doi.org/10.1021/ACSESTAIR.5C00061, 2025.

Ren, H., Li, A., Xie, P., Hu, Z., Xu, J., Huang, Y., Li, X., Zhong, H., Tian, X., Ren, B., Wang, S., and Chai, W.: Investigation of the Influence of Water Vapor on Heavy Pollution and Its Relationship With AOD Using MAX-DOAS on the Coast of the Yellow Sea, Journal of Geophysical Research: Atmospheres, 126, e2020JD034143, https://doi.org/10.1029/2020JD034143;WGROUP:STRING:PUBLICATION, 2021.

Rickards, A. M. J., Miles, R. E. H., Davies, J. F., Marshall, F. H., and Reid, J. P.: Measurements of the sensitivity of aerosol hygroscopicity and the κ parameter to the O/C ratio, J. Phys. Chem. A, 117, 14120–14131, https://doi.org/10.1021/JP407991N, 2013.

Rosenfeld, D., Andreae, M. O., Asmi, A., Chin, M., De Leeuw, G., Donovan, D. P., Kahn, R., Kinne, S., Kivekäs, N., Kulmala, M., Lau, W., Schmidt, K. S., Suni, T., Wagner, T., Wild, M., and Quaas, J.: Global observations of aerosol-cloud-precipitation-climate interactions, https://doi.org/10.1002/2013RG000441, 1 December 2014.

Shen, C., Zhao, G., Zhao, W., Tian, P., and Zhao, C.: Measurement report: Aerosol hygroscopic properties extended to 600 nm in the urban environment, Atmos. Chem. Phys., 21, 1375–1388, https://doi.org/10.5194/acp-21-1375-2021, 2021.

Sjogren, S., Gysel, M., Weingartner, E., Baltensperger, U., Cubison, M. J., Coe, H., Zardini, A. A., Marcolli, C., Krieger, U. K., and Peter, T.: Hygroscopic growth and water uptake kinetics of two-phase aerosol particles consisting of ammonium sulfate, adipic and humic acid mixtures, J. Aerosol Sci., 38, 157–171, https://doi.org/10.1016/J.JAEROSCI.2006.11.005, 2007.

Stokes, R. H. and Robinson, R. A.: Interactions in aqueous nonelectrolyte solutions. I. Solute-solvent equilibria, Journal of Physical Chemistry, 70, 2126–2131, https://doi.org/10.1021/J100879A010/ASSET/J100879A010.FP.PNG_V03, 1966.

Tan, F., Zhang, H., Xia, K., Jing, B., Li, X., Tong, S., and Ge, M.: Hygroscopic behavior and aerosol chemistry of atmospheric particles containing organic acids and inorganic salts, npj Climate and Atmospheric Science 2024 7:1, 7, 1–21, https://doi.org/10.1038/s41612-024-00752-9, 2024.

Vu, T. V., Shi, Z., and Harrison, R. M.: Estimation of hygroscopic growth properties of source-related sub-micrometre particle types in a mixed urban aerosol, NPJ Clim. Atmos. Sci., 4, https://doi.org/10.1038/s41612-021-00175-w, 2021.

Wex, H., Petters, M. D., Carrico, C. M., Hallbauer, E., Massling, A., McMeeking, G. R., Poulain, L., Wu, Z., Kreidenweis, S. M., and Stratmann, F.: Atmospheric Chemistry and Physics Towards closing the gap between hygroscopic growth and activation for secondary organic aerosol: Part 1-Evidence from measurements, Atmos. Chem. Phys, 3987–3997 pp., 2009.

https://doi.org/10.5194/egusphere-2026-1992
Preprint. Discussion started: 30 April 2026

Wu, Z. J., Poulain, L., Henning, S., Dieckmann, K., Birmili, W., Merkel, M., Van Pinxteren, D., Spindler, G., Müller, K., Stratmann, F., Herrmann, H., and Wiedensohler, A.: Relating particle hygroscopicity and CCN activity to chemical composition during the HCCT-2010 field campaign, Atmos. Chem. Phys., 13, 7983–7996, https://doi.org/10.5194/acp-13-7983-2013, 2013.